New methods for calculating the inlet hydrodynamic and thermal length in a laminar nanofluid flow by applying entropy generation theory

M. Boghrati[a], *M. Moghiman*[b]

[a] *Qaen Faculty of Engineering, Birjand University,Qaen, Iran, mboghraty@yahoo.com*
[b] *Ferdowsi University of Mashhad, Mashhad, Iran, mmoghiman@yahoo.com*

Abstract

Several ways have been suggested for obtaining the inlet hydrodynamic and thermal length (l_{hy} and l_{th}). Studying on nanofluid inlet region is more complicated than fully developed region. Blasius, Sparrow, Schlichting, Atkinson and Chen presented different equations due to Reynolds number and diameter of channel to predict l_{hy}. Another method is where maximum velocity reaches to 1.5 times of inlet velocity. In this research the new method due to hydrodynamic entropy generation is presented. The difference between this method and Atkinson equation is 0.8%. Shah and Hanna presented the relations due to Pecklet number and hydraulic diameter of channel to obtain the l_{th}. The other ways to find l_{th} are according to difference of mean temperature and walls temperature, dimensionless temperature and Nusselt number. The new method to predict the l_{th} is due to thermal entropy generation. When the entropy generation approaches to 0.94% of final value, l_{th} value equals to Shah solution.

Keywords:

Nanofluid, inlet length, entropy generation.

1. INTRODUCTION

Using fluid additives is one of the passive heat transfer enhancement techniques. One of the major limits of the heat transfer improvement of heat exchangers is the poor thermophysical properties of conventional heat transfer fluids such as water, ethylene glycol or engine oil. These fluids have much lower thermal conductivity than metallic and metallic oxide solids. For example, the thermal conductivity of aluminum oxide at room temperature is about 67 times greater than that of water and about 275 times greater than that of engine oil. Therefore, it is predictable that the thermal conductivities of fluids containing suspended these solid particles are higher than those of conventional heat transfer fluids. Nanofluids, which are suspensions of nanoparticles in conventional fluids, are very stable and almost free from problems such as sedimentation, channel clogging, extra pressure drop and erosion.

Experimentalists have shown that nanofluids not only have a better thermal conductivity but also have a higher convective heat transfer capability than that of base fluids [1-13]. There are also several numerical studies in convective heat transfer of nanofluids [14-20] which prove the nanofluids convective heat transfer enhancement. It has been shown that nanoparticle shape is a significant parameter in this issue. The study of the nanoparticle shape effects on heat transfer illustrates that the enhancement of both thermal conductivity and convective heat transfer coefficient of nanofluids with the cylindrical nanoparticles is considerably higher than spherical nanoparticles [21-23]. The thermal heat transfer increases with nanoparticle volume fraction; but, the extra pressure drop, or pumping power, will somewhat decrease the positive effects.

The nanofluids have great potential for enhancing heat transfer. However, research work on the concept, enhancement mechanism, and application of the nanofluids is still in the primary stage. To the extent of authors' knowledge, there is no study available on combination of two mentioned passive heat transfer enhancement techniques of using bluff bodies and nanofluids.

Finding or predicting the hydrodynamic and thermal inlet length is so important. The behavior of velocity or nondimensional temperature gradients is different in inlet length and fully developed region. In fully developed region the gradient of velocities and nondimensional temperatures are constant.

In the hydrodynamic inlet region, because of greater cross gradient of axial velocity, the wall bearing tension is maximum. There isn't any precision method to predict the inlet length[24]. In some problems to study on thermal inlet region, at first the flow passes from a thermal insulated wall. Where it reaches to hydrodynamics fully developed region wall thermal condition changes to constant temperature or heat flux. Then we have a hydrodynamic fully developed and thermal developing flow[25].

For the first time Schiller used integral method to study the inlet length.

Blasius [26] equation to predict the hydrodynamic inlet length is:

$$\frac{L_{hy}/D}{\mathrm{Re}_D} = 0.01 \qquad (1)$$

Sparrow [26] suggested the other relation:

$$\frac{L_{hy}/D}{\mathrm{Re}_D} = 0.026 \qquad (2)$$

Schlichting [24] calculated the hydrodynamic inlet length by the approximated relation:

$$\frac{L_{hy}/D}{\mathrm{Re}_D} = 0.04 \qquad (3)$$

Atkinson [25] suggested the next equation:

$$L_{hy}/D_h = 0.3125 + 0.011\,\mathrm{Re} \qquad (4)$$

Chen [27] provided the last equation:

$$\frac{L_{hy}}{D_h} = \frac{0.315}{0.0175\,\mathrm{Re}+1} + 0.011\,\mathrm{Re} \qquad (5)$$

In current Numerical solution the maximum velocity is observed. Where the velocity at the centre of the channel reaches to $0.99U_{max}$, fully developed region occurs [26].

For thermal inlet length some solutions have been provided. Shah [28] suggested two relations to find inlet thermal length in wall temperature constant and heat flux constant. They are presented in equations 6 and 7 respectively:

$$L^*_{th,T} = \frac{L_{th}}{D_h Pe} = 0.0079735 \qquad (6)$$

$$L^*_{th,H} = \frac{L_{th}}{D_h Pe} = 0.0115439 \qquad (7)$$

Hanna [29] obtained thermal inlet length for constant heat flux by the next equation:

$$L^*_{th,H} = \frac{L_{th}}{D_h Pe} = 0.00871 \qquad (8)$$

The next way to predict the thermal inlet length is nondimensional temperature [26].

$$\theta = \frac{T - T_w}{T_m - T_w} \qquad (9)$$

$$T_m = \frac{1}{U_{in} H} \int_0^H uTdy \qquad (10)$$

Where T_w is wall temperature, T_m is mean temperature and u_{in} is the uniform inlet velocity. In fully developed thermally region the nondimensional temperature is constant. Where the nondimensional temperature of channel center reaches to 0.99 of final value fully developed region begins.

Another solution is Nusselt number. In parallel plate channel with constant heat flux, the final value of Nusselt number is 8.235[26]. Fully developed region is where the amount of Nusselt number reaches to 0.99 of final value [30].

The next solution is the difference of mean temperature (T_m) and wall temperature (T_w)[30]. When the difference of them becomes constant the thermal fully developed occurs.

In this study new methods are suggested to predict inlet hydrodynamic and thermal inlet length. These methods base on entropy generation theory. The results are comprised with other solutions. The results show that these methods are so predictable.

2. Mathematical Modelling

It is assumed that the fluid phase and nanoparticles are in thermal equilibrium with zero relative velocity. The governing equations are the incompressible Navier–Stokes and energy equations in integral form as:

$$\iint \rho_e \vec{V} \cdot d\vec{A} = 0 \qquad (11)$$

$$\iint \vec{V} \rho_e \vec{V} \cdot d\vec{A} = -\iint P \vec{n} \cdot d\vec{A} + \iint \mu_e \vec{\nabla} \vec{V} \cdot d\vec{A} \qquad (12)$$

$$\iint \left(\rho C_p\right)_e T \vec{V} \cdot d\vec{A} = \iint k_e \vec{\nabla} T \cdot d\vec{A} \qquad (13)$$

Where, $\vec{V}$, P and T are the velocity vector, pressure, and temperature. $\vec{A}$ and $\vec{n}$ represent the cross-section area and its normal unit vector respectively. Also, ρ_e, k_e, μ_e, and Cp_e are density, thermal conductivity, viscosity and heat capacity of nanofluid, respectively, where the subscript e indicates effective properties of nanofluids defined as:

Density:

$$\rho_e = (1-\phi)\rho_f + \phi\rho_p \qquad (14)$$

Heat capacity:

$$Cp_e = \frac{(1-\phi)(\rho Cp)_f + \phi(\rho Cp)_p}{(1-\phi)\rho_f + \phi\rho_p} \qquad (15)$$

Entropy Generation[31]:

$$S'''_{gen} = \frac{k}{T^2}\left[\left(\frac{\partial T}{\partial x}\right)+\left(\frac{\partial T}{\partial y}\right)\right]+ 2\frac{\mu}{T}\left\{\left(\frac{\partial u}{\partial x}\right)^2+\left(\frac{\partial u}{\partial y}\right)^2+\left(\frac{\partial u}{\partial y}+\frac{\partial \upsilon}{\partial y}\right)^2\right\} \quad (16)$$

The first term on the right-hand side of the above equation is Thermal Entropy Generation (TEG) and the second term is Viscous Entropy Generation (VEG).

For the incompressible, 2D flow in the channel described above, the dimensionless form of the continuity, the *x* and *y* components of the Navier-Stokes, and the thermal energy equation were solved numerically in a rectangular coordinate system and are given below [26].

Continuity:

$$\frac{\partial U}{\partial X}+\frac{\partial U}{\partial Y}=0 \quad (17)$$

Momentum:

$$U\frac{\partial U}{\partial X}+V\frac{\partial U}{\partial Y}=-\frac{1}{\rho}\frac{\partial P}{\partial X}+V\left(\frac{\partial^2 U}{\partial X^2}+\frac{\partial^2 U}{\partial Y^2}\right) \quad (18)$$

$$U\frac{\partial V}{\partial X}+V\frac{\partial V}{\partial Y}=-\frac{1}{\rho}\frac{\partial P}{\partial Y}+V\left(\frac{\partial^2 V}{\partial X^2}+\frac{\partial^2 V}{\partial Y^2}\right) \quad (19)$$

Energy:

$$U\frac{\partial \theta}{\partial X}+V\frac{\partial \theta}{\partial Y}=\alpha\left(\frac{\partial^2 \theta}{\partial X^2}+\frac{\partial^2 \theta}{\partial Y^2}\right) \quad (20)$$

Where the following dimensionless variables are used:

$$U=\frac{u}{u_\infty},\ V=\frac{\upsilon}{u_\infty},\ X=\frac{x}{L},\ Y=\frac{y}{H},\ \theta=\frac{T-T_\infty}{q_w L/k}$$

3. Numerical Approach

The governing equations were solved using finite volume method and SIMPLE algorithm and since Pe>2, the upwind scheme is employed [32]. The convergence criterion was the residuals (R) of energy and momentum equations to become 0.001 of the order of each amount. R is defined as follows:

$$R=\sum_{i=1}^{mx}\sum_{j=1}^{my}\left(\phi(i,j)_{new}-\phi(i,j)_{old}\right) \quad (21)$$

In which ϕ is θ, U or V. In order to validate the results, the Nusselt number for the channel with constant heat flux was calculated and compared the well-known value of 8.235.

$$\mathrm{Nu}=\left(\left.\frac{\partial T}{\partial y}\right|_{y=0 \text{ or } H}\right)D_h \Big/ (T_w-T_m) \quad (22)$$

The physical domain was discretized with different non-uniform grids of 201×123 with expansion coefficient 1.05 and 24723 nodes.

4. Results and Discussions

4.1. Hydrodynamic inlet length

Fig. 1 shows the comparison of current solutions. In the Re<100 the numerical solution is adapted with Atkinson, Chen and Sparrow solutions. For Re>100 it's adapted with Schlichting solution.

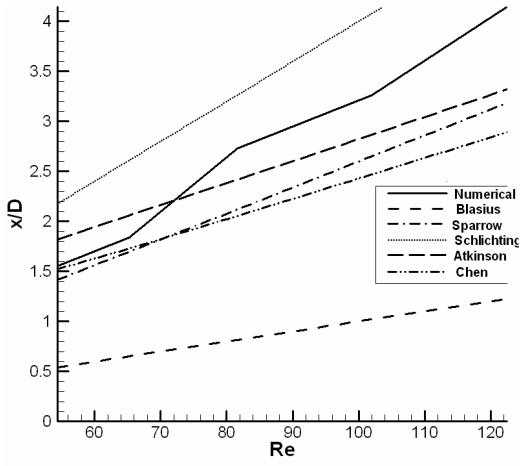

Fig. 1. Nondimensional hydrodynamic inlet length vs. Reynolds number.

In this method the term of viscous entropy generation is observed.:

$$fi = \frac{\mu}{T}\left\{2\left[\left(\frac{\partial u}{\partial x}\right)^2 + \left(\frac{\partial v}{\partial y}\right)^2 + \left(\frac{\partial u}{\partial y} + \frac{\partial v}{\partial x}\right)^2\right]\right\} \quad (23)$$

Table 1. Thermophysical properties

Water / CNT $\phi = 0.5\%$	Property
1008	$\rho(kg.m^{-3})$
4134	$Cp(J.kg^{-1}.K^{-1})$
0.87×10^{-3}	$\mu(Pa.s)$
3.7	$k(W.m^{-1}.K^{-1})$
0.97	Pr

As shown in the equation 23 velocity gradients effected on the value of viscous entropy generation. Fully developed region where occurs that the velocity profiles become constant. In the viscous entropy generation term all the velocity gradients are present. In this region the velocity only varies in y direction and the value is constant. So where fi becomes constant fully developed region occurs. In this method all of velocity gradients are considered but in the current solutions all velocity gradients aren't considered. So the precision of this method is higher than the others. Fig. 2 shows the viscous entropy generation along the flow.

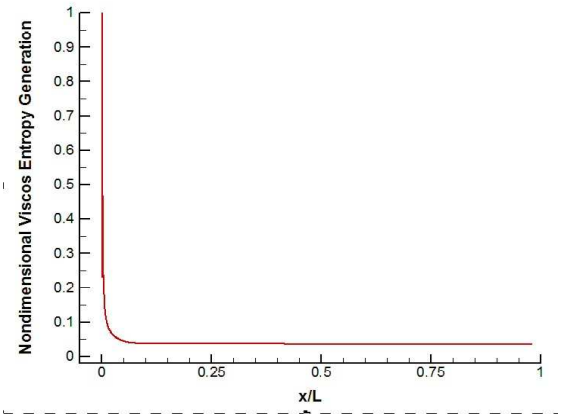

Fig. 2. Viscous entropy generation vs. channel length.

The comparison of result of this method with others is presented in table 2. All amounts are constant for all cases. The result of new method is so adapted with current solutions and because of considering all of velocity gradients, is so precise.

$D = 0.05m \rightarrow D_h = 0.1m$,Re_D=80.549

Table 2: Hydrodynamic inlet lengths for different methods

Solutions	L_{hy} (m)
Blasius	0.081
Sparrow	0.21
Schlichting	0.32
Atkinson	0.12
Chen	0.1
Numerical	0.16
Viscous Entropy generation	0.47

4.2. Thermal inlet length

The new method to predict thermal inlet length is thermal entropy generation:

$$S'''_{gen,T} = \frac{k}{T^2}\left[\left(\frac{\partial T}{\partial x}\right)^2 + \left(\frac{\partial T}{\partial y}\right)^2\right] \quad (24)$$

In this term all the temperature gradients are considered. When the nondimensional temperature becomes constant the thermal fully developed region occurred. The nondimensional temperature only varies in y direction and the value is constant.

All the flow parameters are constant for all cases:

Pe=78.73, Re=80.549, Pr=0.977, D_h=0.1 m

The thermal entropy generation along the flow direction is shown in Fig. 3.

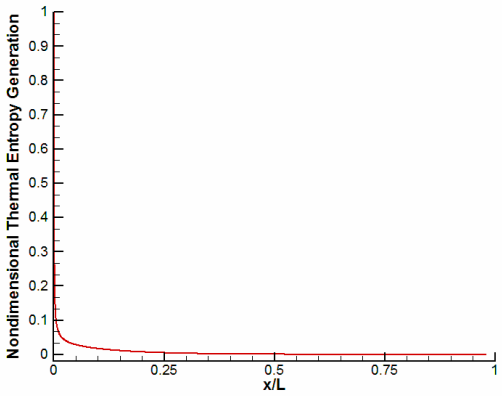

Fig. 3. Thermal entropy generation along flow direction.

According to Fig. 3, in thermal fully developed region the entropy generation value tends to a constant amount. In Shah [28] solution L_{th}=0.091. In new method where the nondimensional thermal entropy generation reaches to 0.02 then L_{th}= 0.091.

The comparison between all cases is presented in table 3.

Table 3. Thermal inlet length in all solutions

Solutions	L_{th} (m)
Shah	0.091
Hanna	0.069
Nondimensional Temperature	0.585
T_m-T_w	0.6
Thermal entropy generation	0.549

5. Conclusion

Maximum viscous entropy generation is in the inlet of channel. It decreases along the flow direction till it tends to a constant value. The zone of constant value is fully developed region. In this method all gradients of velocities are considered. So the precision of this method is higher than the others. The new method to predict the lth is due to thermal entropy generation. In thermal fully developed region temperature gradients are constant. So the thermal entropy generation becomes constant. Comparison between new method and current procedures indicates that this method is so predictable.

6. Nomenclature

A Area (m^2)

C_p specific heat (kJ/kg.K)

CNT Carbon NanoTube

D_h hydraulic diameter (m)

h block height (m)

H channel height (m)

k thermal conductivity of fluid (W/m K)

L channel length (m)

n normal unit vector

Nu Nusselt number defined in eq. 7

P Pressure (kPa)

Pr Prandtl number = v/α

Re Reynolds number = $\rho u D_h/\mu$

S'''_{gen} entropy generation per unit volume defined in eq. 16 (J/K.m^3)

T temperature (K)

TEG Thermal Entropy Generation

u, υ velocity components in the *x* and *y* directions (m/s)

VEG Viscous Entropy Generation

w block length (m)

x, y rectangular coordinate system (m)

Greek symbols

β blockage ratio = h/H

μ dynamic viscosity (kg/ms)

Φ volume fraction of nanoparticles

ρ density

Subscripts

e effective properties of nanofluids

f fluid

m mean

out outlet

p particle

s block center

w wall

∞ inlet flow

7. References

[1] Li Q, Xuan Y. Convective Heat Transfer and Flow Characteristics of Cu-Water Nanofluid. Science in China (Series E) 2002;45(4):408-416.

[2] Wen D, Ding Y. Experimental Investigation Into Convective Heat Transfer of Nanofluids at the Entrance Region Under Laminar Flow Conditions. Int. J. Heat Mass Transfer 2004;47:5181-5188.

[3] Yang Y, Zhang ZG, Grulke EA, Anderson WB, Wu G. Heat Transfer Properties of Nanoparticle-in-Fluid Dispersions (Nanofluids) in Laminar Flow. Int. J. Heat Mass Transfer 2005;48(6):1107-1116.

[4] Yulong Ding, Dongsheng Wen. Particle migration in a flow of nanoparticle suspensions. Powder Technology 2005;149:84-92.

[5] Ding Y, Alias H, Wen D, Williams R A. Heat Transfer of Aqueous of Carbon Nanotubes (CNT Nanofluids). Int. J. Heat Mass Transfer 2006;49:240-250.

[6] Heris S Z, Esfahany M N, Etemad G. Investigation of CuO/Water Nanofluid Laminar Convective Heat Transfer through a Circular Tube. J. Enhanced Heat Transfer 2006;13(4):279-289.

[7] Zeinali Heris S, Etemad S Gh, Nasr Esfahany M. Experimental investigation of oxide nanofluids laminar flow convective heat transfer. International Communications in Heat and Mass Transfer 2006;33:529-535.

[8] He Y, Jin Y, Chen H, Ding Y, Chang D, Lu H. Heat Transfer and Flow Behavior of Aqueous Suspensions of TiO2 Nanoparticles Nanofluids Flowing Upward Through a Vertical Pipe. Int. J. Heat Mass Transfer 2007;50:2272-2281.
[9] Heris S Z, Esfahany M N, Etemad S Gh. Experimental Investigation of Convective Heat Transfer of Al2O3/Water Nanofluid in Circular Tube. Int. J. Heat Fluid Flow 2007;28(2):203-210.
[10] Akbarinia A, Behzadmehr A. Numerical study of laminar mixed convection of a nanofluid in horizontal curved tubes. Applied Thermal Engineering 2007;27:1327-1337
[11] Mirmasoumi S, Behzadmehr A. Numerical study of laminar mixed convection of a nanofluid in a horizontal tube using two-phase mixture model. Applied Thermal Engineering 2008;28:717-727.
[12] Mirmasoumi S, Behzadmehr A. Effect of nanoparticles mean diameter on mixed convection heat transfer of a nanofluid in a horizontal tube. International Journal of Heat and Fluid Flow 2008;29:557-566.
[13] Akbari M, Behzadmehr A, Shahraki F. Fully developed mixed convection in horizontal and inclined tubes with uniform heat flux using nanofluid. International Journal of Heat and Fluid Flow 2008;29:545-556.
[14] Akbarinia A. Impacts of nanofluid flow on skin friction factor and Nusselt number in curved tubes with constant mass flow. International Journal of Heat and Fluid Flow 2008;29:229-241.
[15] Chen H, Yang W, He Y, Ding Y, Zhang L, Tan Ch, Lapkin A A, Bavykin D V. Heat transfer and flow behaviour of aqueous suspensions of titanate nanotubes (nanofluids). Powder Technology, 2008;183:63-72.
[16] Hwang, K S, Jang S P, Choi S. Flow and convective heat transfer characteristics of water-based Al2O3 nanofluids in fully developed laminar flow regime. International Journal of Heat and Mass Transfer 2008;52:193-199.
[17] Lai W Y, Vinod S, Phelan P E, Prasher R. Convective Heat Transfer for Water-Based Alumina Nanofluids in a Single 1.02-mm Tube. Journal of Heat Transfer 2009;131:112401-1/9.
[18] Anoop K B, Sundararajan T, Das S K. Effect of particle size on the convective heat transfer in nanofluid in the developing region. International Journal of Heat and Mass Transfer 2009;52:2189-2195
[19] Santra A K, Sen S, Chakraborty N. Study of heat transfer due to laminar flow of copper–water nanofluid through two isothermally heated parallel plates. International Journal of Thermal Sciences 2009;48:391-400.
[20] He Y, Men Y, Liu X, Lu H, Chen H, Ding Y. Study on Forced Convective Heat Transfer of Non-Newtonian Nanofluids. Journal of Thermal Science 2009;18(1):20-26.
[21] Murshed S M S, Leong K C, Yang C. Enhanced Thermal Conductivity of TiO2-Water-Based Nanofluids. International Journal of Thermal Sciences 2005;44:367-373.
[22] Murshed S M S, Leong K C, Yang C. Investigations of thermal conductivity and viscosity of nanofluids. International Journal of Thermal Sciences 2008;47:560-568.
[23] Maiga, S.E.B., Palm, S.J., Nguyen, C.T., Roy, G. and Galanis, N., 2005, "Heat Transfer Enhancement by Using Nanofluids in Forced Convection Flows," International Journal of Heat and Fluid Flow, **26**, pp. 530-546.
[24] Schlichting H. Boundary layer theory. New York: John Willey and Sons, McGraw Hill, 1968.
[25] Atkinson B, Brocklebank M P, Card C C H, Smith J M. Low Reynolds number developing flow. AICHE 1969, J.15, 548-553.
[26] Bejan A. Convection heat transfer. New York: John Willy and Sons, 1982.
[27] Chen R Y. Flow in entrance regin at low Reynolds number. Fluids eng. 1973;95:153-158.
[28] Shah R K, London A L. Laminar flow forced convection in ducts. Academic Press; 1978.
[29] Hanna O T, Sandall O C, Paruit B A. Thermal entrance length for laminar flow in various ducts for constant surface heat flux Heat and mass transfer 1976, 3, 89-98.

[30] Incropera F P, DeWitt D P. Introduction to heat transfer. New York: John Willey and Sons, McGraw Hill, 1996.
[31] Bejan A. Entropy generation through heat and fluid flow. New York: John Willey and Sons, McGraw Hill, 1982.
[32] Patankar S V. Numerical heat transfer and fluid flow. Hemisphere, Washington: 1980.